



Extraction of Aluminum from Coal Fly Ash Using Pressurized Sulfuric Acid Leaching with Emphasis on Optimization and Mechanism

PENG WANG,^{1,4} HUIYONG LIU,¹ FANGYAN ZHENG,¹
YUE LIU,¹ GE KUANG ^{1,5} RONGDONG DENG,² and HUAN LI³

1.—College of Chemical Engineering, Fuzhou University, Fuzhou 350108, People's Republic of China.
2.—College of Zijing Mining, Fuzhou University, Fuzhou 350108, People's Republic of China.
3.—Western Australian School of Mines: Minerals, Energy and Chemical Engineering, Curtin University, Bentley, WA 6102, Australia. 4.—e-mail: 1961926038@qq.com.
5.—e-mail: kuangge1970@sina.com

Coal fly ash, commonly produced from thermal power plants, is not only an industrial waste but an aluminum-rich resource that needs to be disposed of properly. This study aims to extract aluminum from coal fly ash using pressurized sulfuric acid (H_2SO_4) leaching and to investigate the dissolution mechanism during the leaching process. The effects of initial concentration of H_2SO_4 , reaction temperature and time on the extraction of aluminum were investigated. Under optimized conditions (3 mol/l H_2SO_4 , 220°C and 180 min), the extraction of aluminum reached 82.51%. It was found that mullite ($3\text{Al}_2\text{O}_3 \cdot 2\text{SiO}_2$) contained in coal fly ash was completely dissolved during the leaching, while the dissolution of silica-alumina glass beads was at a limited degree. The un-leached aluminum was found to be locked inside the glass beads which H_2SO_4 was unable to access.

INTRODUCTION

Coal fly ash (CFA) is an industrial solid waste mostly produced from thermal power plants. The appropriate disposal of CFA has gained intensive attention as the landfill of such waste will not only consume a large area of land but also cause high risks to human health and the environment.¹ In particular, CFA has been used in subgrade backfilling, construction materials, glass ceramics and soil improvement.^{2–6} In addition, CFA has shown promising potential as an alternative to Portland cement used in concrete.^{7,8} By adding CFA, the pore structure of hardened cement can be significantly improved, resulting in higher strength and durability of concrete.⁹ However, the considerable amount of aluminum (Al) contained in CFA (averagely 30 wt.% Al_2O_3) has not been widely utilized.¹⁰ The recovery of Al from CFA, therefore, becomes important for both economic and environmental reasons.

This is particularly valued by countries like China which heavily rely on the import of bauxite for the aluminum industry.

Currently, the methods reported for the extraction of Al from CFA can be categorized as (1) high-temperature roasting,^{11–18} (2) sequential acid/alkali treatments^{17–21} and (3) acid leaching.^{22–26} High-temperature roasting (> 700°C) has been reported to have high Al extraction (> 90%) but it requires high energy consumption and could even produce a higher amount of solid waste compared with the original CFA. Sequential acid/alkali treatments inevitably need high consumption of both acid and alkali with high costs. In contrast, acid leaching presents the advantage of lower operating temperature (< 350°C), and it is beneficial for low-iron and high-silicon minerals of CFA as silicon is resistant to common mineral acids (except hydrofluoric acid). However, Al extraction using acid leaching is currently much lower than that using high-temperature roasting. To improve this, some researchers have added fluorides into the leaching system to in situ generate hydrofluoric acid (capable of

destroying Si–Al bond).²⁷ As a result, the Al extraction can be increased up to 90–95%.²⁷ The hydrochloric acid leaching process is advantageous mainly for its low reaction temperature, leading to a lower energy consumption.²⁸ However, as a reaction medium, the obvious volatilization of hydrochloric acid restricts its application ranges. In addition, there have been reports of employing pressure while acid leaching to intensify Al extraction from CFA.^{24,26} Unfortunately, the leaching mechanism has not been detailed yet.

Therefore, in the present study, sulfuric acid leaching under pressure was employed to extract Al from CFA. Based on previous studies, the leaching conditions were further optimized to achieve a satisfactory Al extraction. It is expected that this study could show the potentials of pressurized acid leaching, and the illustrated leaching mechanisms could provide a better understanding of the process and guide the further development of the method.

EXPERIMENTAL

Materials and Reagents

The CFA sample used in this study was supplied by Datang Tuoketuo thermal power plant (Inner Mongolia, China). As shown in Table I, the sample contained 50.11% SiO₂ and 30.63% Al₂O₃. The XRD analysis (Fig. 1) indicates that the CFA was mainly composed of mullite (3Al₂O₃·2SiO₂), quartz (SiO₂) and anhydrite (CaSO₄). The analysis of particle size distribution (Fig. 2) indicates a D90 value of 153.76 μm.

The concentration of sulfuric acid (H₂SO₄) used in this study was 98 wt.%. All other chemicals were of analytical grade. De-ionized (DI) water was used to prepare leaching solution and to dilute solution samples for analysis.

Experimental Procedures

Leaching experiments were performed by mixing 5.0 g CFA, a certain amount of H₂SO₄ and DI water in a high-pressure reaction kettle (KFC, Beijing Century Senlong Experimental Apparatus Co., Ltd., Beijing, China). The mass ratio of CFA and H₂SO₄ was fixed depending on the metal oxides contained in CFA. The mixture was then digested at a

temperature of 160–260°C for a certain period (30–180 min). After cooling with cold water, the leachate and residue were separated by vacuum filtration. The residue was then washed with hot water (80–90°C) and dried at 105°C for 24 h for further instrumental analyses.

Characterizations

Various instrumental analyses were carried out for the characterization of CFA and leaching residues, including particle size distribution (Mattersizer 2000, Malvern Instruments Co., Ltd, UK), x-ray diffraction (XRD, PANalytical-X'Pert PRO, The Netherlands) and scanning electron microscopy (SEM, Helios G4 CX, USA). The specific surface area and pore size distributions of the samples were determined using the Accelerated Surface Area and Porosimetry System (ASAP 2460, USA).

EDTA complexometric titration method was used to determine Al concentration in solution samples.¹² Other elements were quantitatively analyzed by plasma emission spectrometer (iCAP7400, Thermo Fisher Scientific, USA).²⁰

Al extraction presented in this study was calculated by:

$$\mu = \frac{m_1\omega_1 - m_2\omega_2}{m_1\omega_1} \quad (1)$$

where μ is the extraction of Al, %; m_1 is the mass of CFA before leaching, g; ω_1 is the content of Al in CFA, %; m_2 is the mass of the residue after leaching, g; ω_2 is the content of Al in residue, %.

RESULTS AND DISCUSSION

Optimal Leaching Conditions

Effect of Temperature

To investigate the effect of leaching temperature (T, 160–260°C) on extraction, several experiments were performed at 1.2 mol/L H₂SO₄, 10 mL/g liquid-solid (L/S) ratio for 120 min. The results, shown in Fig. 3a, indicate that temperature had a considerable effect on the extraction of Al. When the temperature was increased from 160 to 220°C, Al extraction was almost doubled from 33.87 to 62.71%. However, further increase of temperature showed detrimental effect on Al extraction. To

Table I. Chemical composition of CFA (%), residue (%) and filtrate (g/L)

| Sample | SiO ₂ | Al ₂ O ₃ | CaO | Fe ₂ O ₃ | MgO | TiO ₂ | K ₂ O |
|----------|------------------|--------------------------------|------|--------------------------------|------|------------------|------------------|
| CFA | 50.11 | 30.63 | 7.69 | 4.88 | 1.52 | 1.13 | 0.93 |
| Residue | 76.90 | 8.14 | 4.60 | 1.53 | 0.37 | 1.25 | 0.77 |
| Filtrate | ND | 19.35 | 3.47 | 6.26 | 1.54 | 0.10 | 0.17 |

ND Not detected.

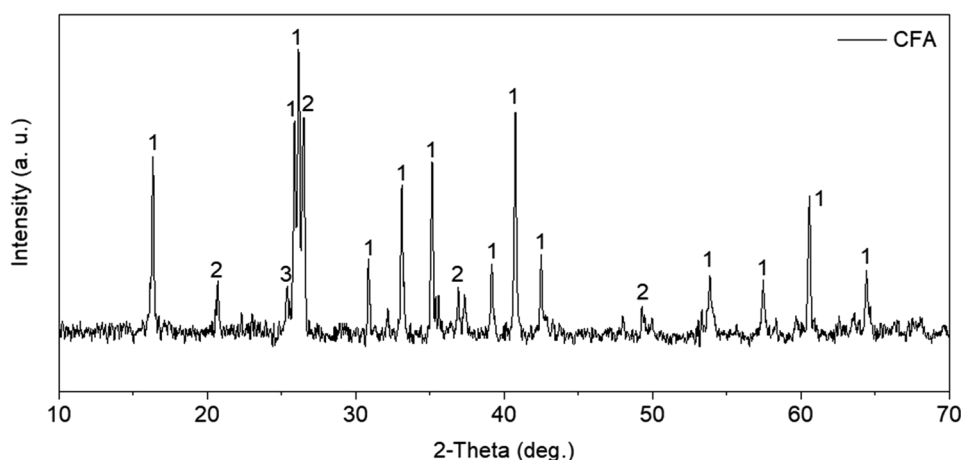


Fig. 1. XRD analysis of the CFA. 1: mullite, 2: quartz, 3: anhydrite.

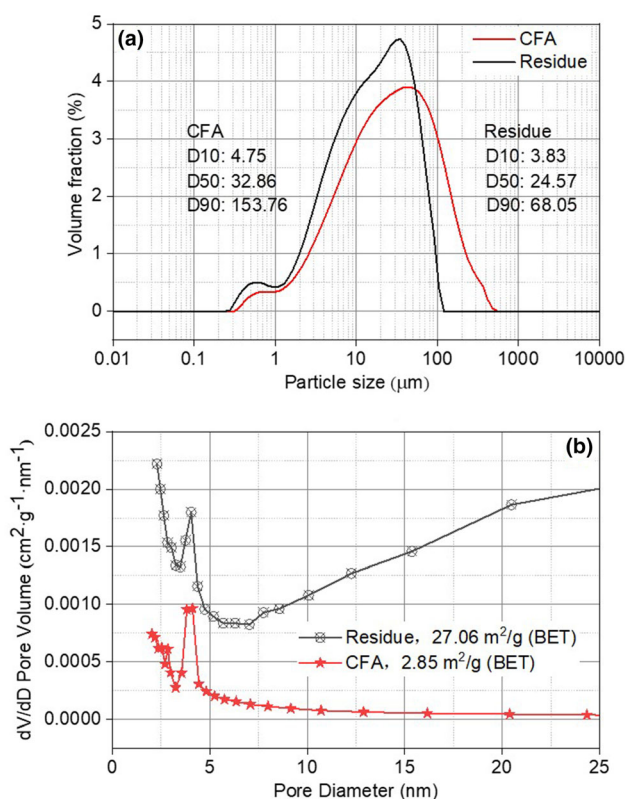


Fig. 2. (a) Particle size distribution and (b) pore diameter distribution of CFA and residue.

explain this, XRD analysis of the leaching residues (Fig. 4a) was performed. It can be seen that a new phase of hydronium alunite ($(\text{H}_3\text{O})\text{Al}_3(\text{SO}_4)_2(\text{OH})_6$, ICDD; 016-0409²⁹) was detected at 240°C and 260°C, which did not happen to the residues from the leaching at lower temperatures. The formation of the insoluble hydronium alunite explains the decrease of Al leaching when the temperature was beyond 220°C.

The pressure of the reactor was monitored (by gauge) and is shown in Fig. 3a, L2. It is reasonable that higher pressure was recorded while system temperature was increasing. The saturated vapor pressure of the system was calculated by Eq. (2)³⁰ and plotted as L2 in Fig. 3a, which was found to be consistent with the monitored pressure of L1.

$$\ln(0.1p) = 12.062 - \frac{4039.558}{T + 235.379} \quad (2)$$

where p represents the pressure (Mpa), and T is the temperature (°C), respectively. For the consideration of safety and energy consumption, the leaching temperature of 220°C was selected for the following experiments and pressure was about 2.2 Mpa in this temperature.

Effect of Initial H_2SO_4 Concentration

Several experiments were conducted to investigate the effect of initial H_2SO_4 concentration (1–5 mol/L) on Al extraction at L/S ratio of 10 mL/g and 220°C for 120 min. As revealed in Fig. 3b, when the initial H_2SO_4 concentration increased from 1 to 3 mol/L, the Al extraction jumped by about 31%. However, the further increase of concentration did not lead to a considerable increase of Al extraction.

The XRD patterns of the original CFA and residues are shown in Fig. 4b. It can be seen that hydronium alunite was formed and the diffraction peaks intensity of anhydrite increased compared with CFA at 1 mol/L. When the acid concentration was at 2 mol/L, the hydronium alunite disappeared and the diffraction peaks intensity of anhydrite decreased above 2 mol/L, until completely disappearing at 4 mol/L. The diffraction peak intensity of mullite became weaker as the concentration of acid was raised. The change of phase composition in leached residue reveals that mullite tends to decompose at a high concentration of sulfuric acid because the contact chance between H^+ and CFA increases with increasing acid concentration.

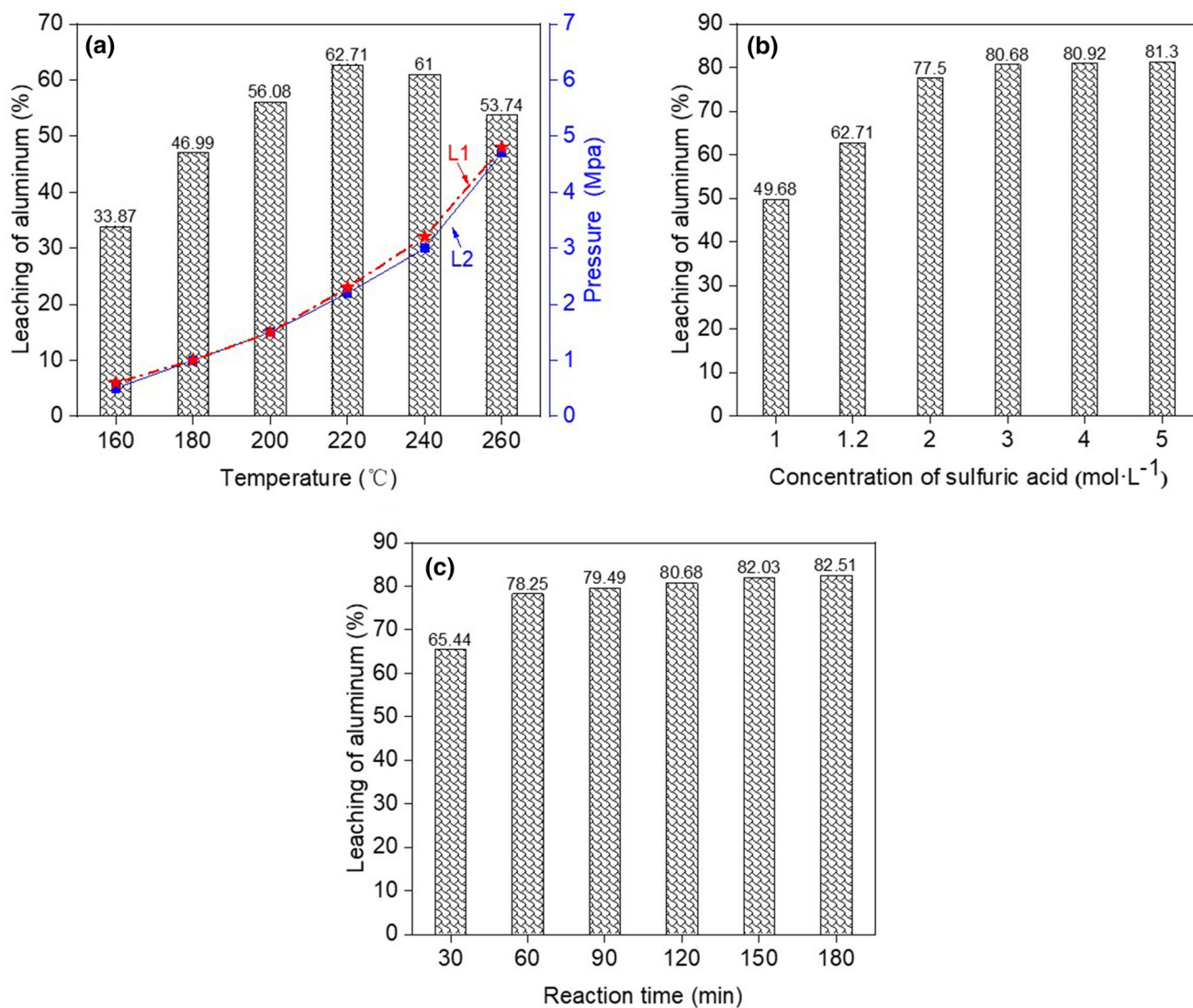


Fig. 3. Effect of (a) temperature, (b) initial H_2SO_4 concentration and (c) reaction time on the leaching of Al (L1, saturated vapor pressure curve; L2, measured pressure curve)

Effect of Reaction Time

Figure 3c shows the effect of reaction time in the range of 30–180 min on the extraction of Al at initial H_2SO_4 concentration of 3 mol/L and 220°C. Al extraction increased rapidly from 65.44 to 80.68% when the time increased from 30 to 120 min, while the further increase of time led to slower kinetics of Al extraction.

XRD analysis of the obtained residues was then performed to further investigate the effect of time. As Fig. 4c shows, diffraction peaks of mullite disappeared at 60 min, and anhydrite was identified in the residues from 120–180 min but not from a shorter time of 60–90 min. Moreover, the characteristic peak strength of anhydrite in the residue was higher for a reaction time of 180 min. This indicates a lower level of calcium ions was leached into the solution, which could facilitate the

downstream separation and purification process. Therefore, the optimized reaction time was selected as 180 min.

At a sulfuric acid concentration of 3 mol/L, leaching time of 180 min and leaching temperature of 220°C, the filtrate was analyzed, as shown in Table I. The concentration of alumina in the filtrate reached as high as 19.35 g/L, which can be used to prepare other Al products, such as aluminum potassium sulfate ($\text{KAl}(\text{SO}_4)_2 \cdot 12\text{H}_2\text{O}$).^{31,32}

SEM-EDS Analysis

To get a clearer observation of the glass beads during pressure leaching by sulfuric acid, CFA and the residues were characterized by SEM-EDS, and the results are shown in Fig. 5. Figure 5a shows that both Si and Al were widely distributed on the surface of CFA. However, after pressure leaching by

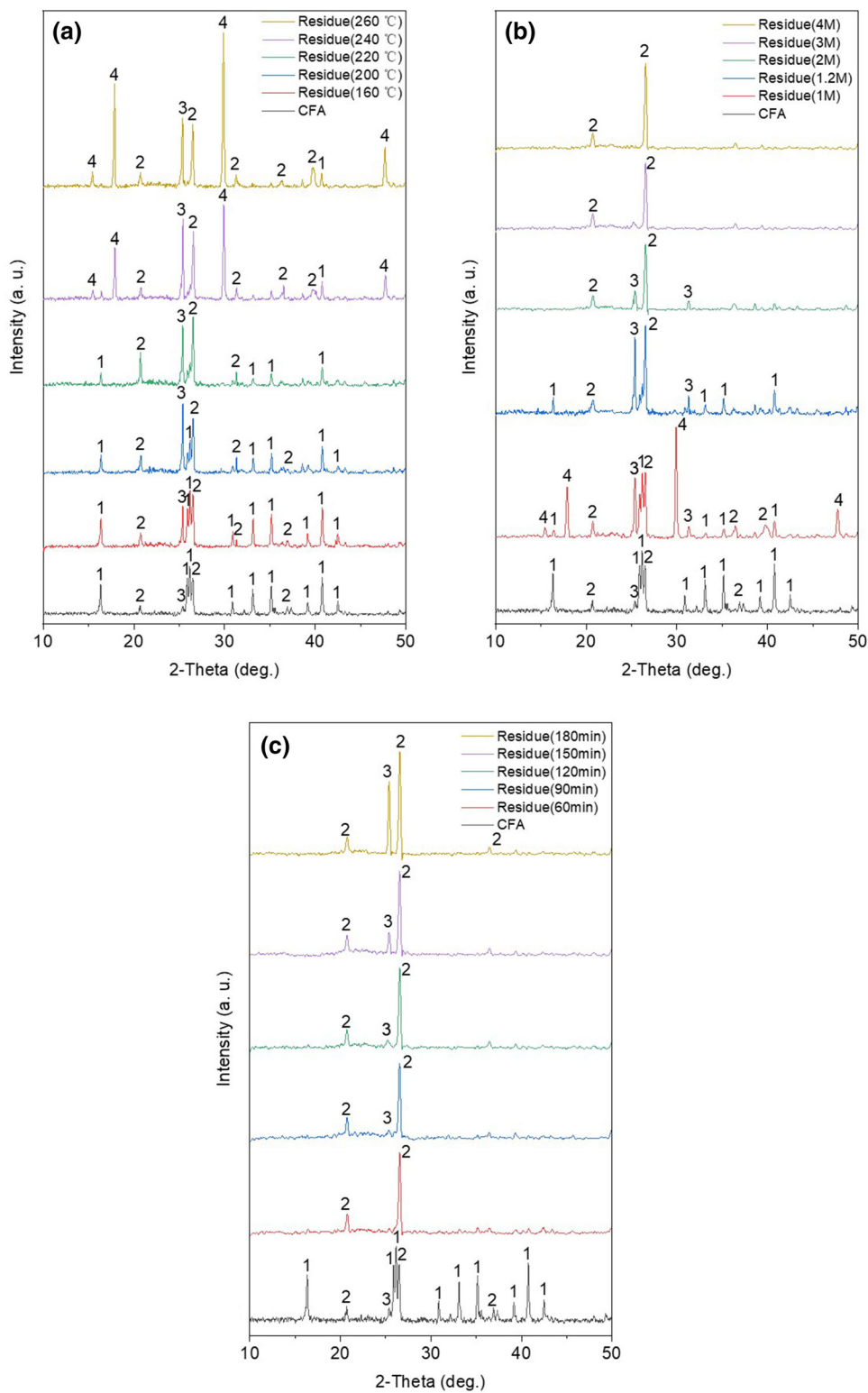


Fig. 4. XRD pattern: (a) variable by temperature, (b) variable by initial H₂SO₄ concentration and (c) variable by reaction time. (1: mullite, 2: quartz, 3: anhydrite, 4: hydronium alunite)

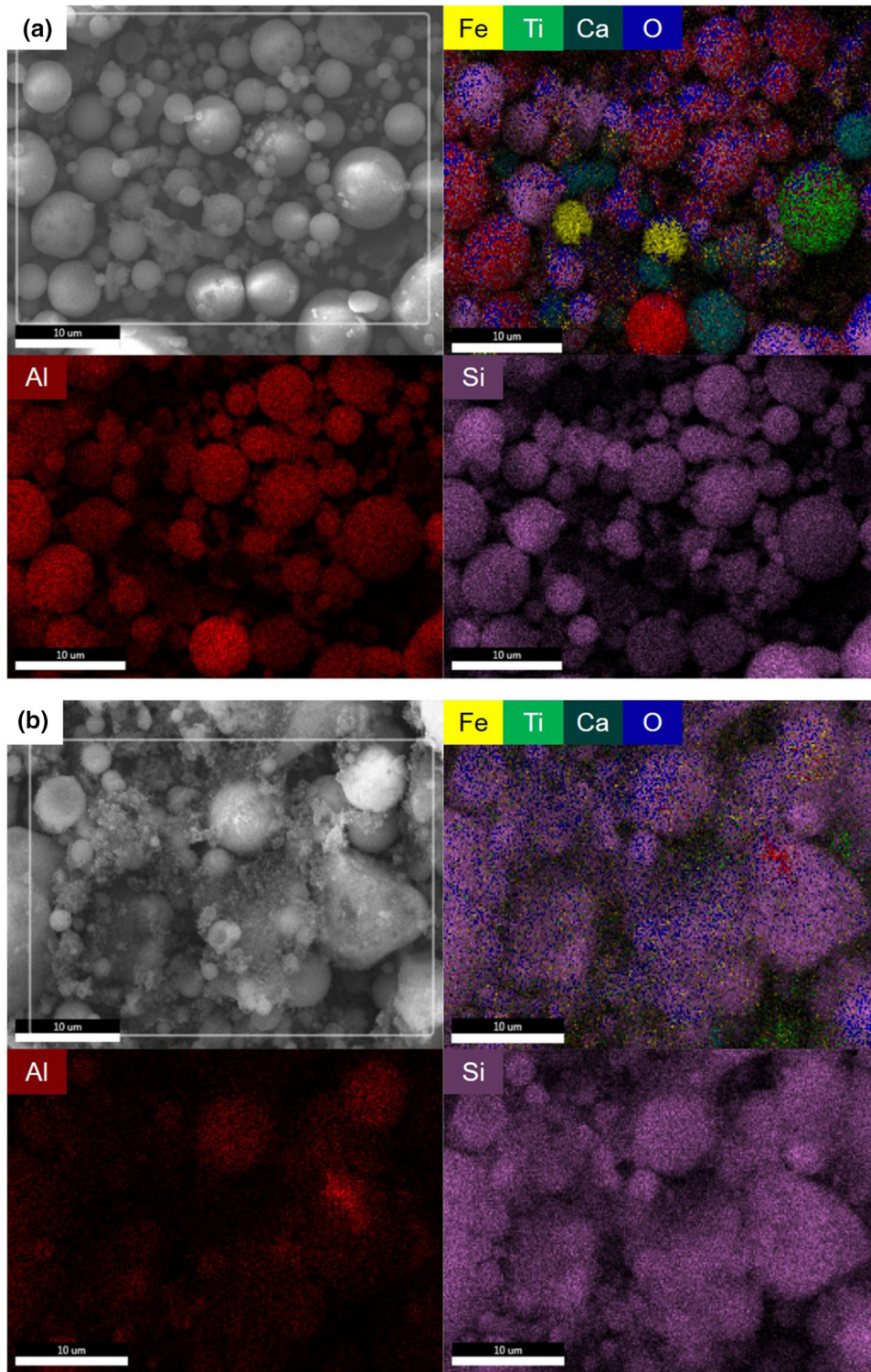


Fig. 5. SEM elemental maps for main elements on the surface of (a) CFA and (b) residue. (Residue obtained at 220°C, 3 mol/L H_2SO_4 and 180 min)

H_2SO_4 , the amount of Si on the surface of the residue increased sharply, along with a clear decrease of the amount of Al (Fig. 5b). This indicates that the Al distributed on the particle surface was preferentially dissolved by H_2SO_4 solution, and a

large amount of Si was hence accumulated on the particle surface.

To further explore the leaching behavior of the glass beads before and after H_2SO_4 leaching, the beads were cut for cross-section analysis by SEM-

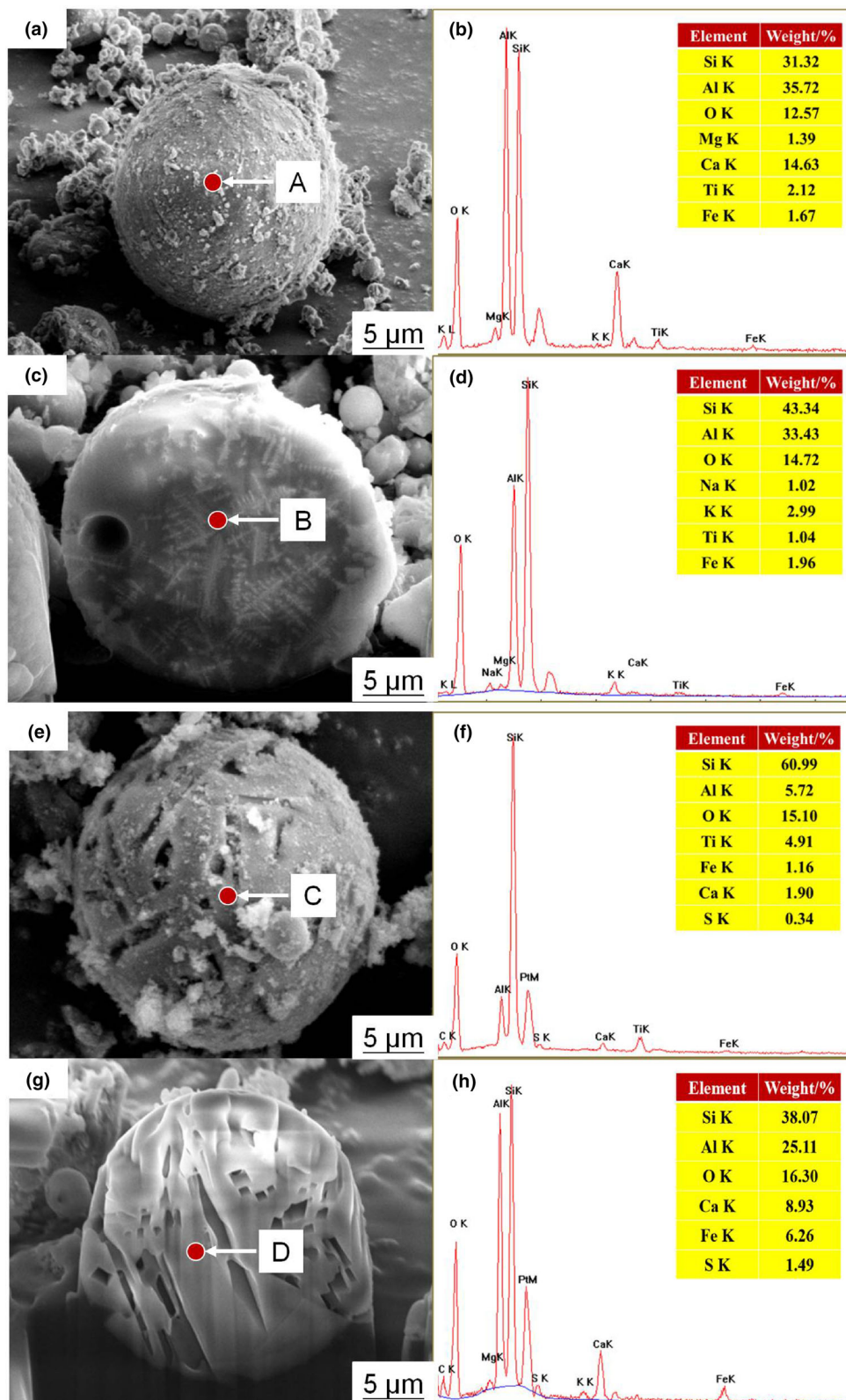


Fig. 6. Analysis of SEM elemental point for main elements of samples. (Residue obtained at 220°C, 3 mol/L H₂SO₄ and 180 min). (a) SEM of glass bead from CFA; (b) EDS of point A; (c) SEM of glass bead's section from CFA; (d) EDS of point B; (e) SEM of glass bead from residue; (f) EDS of point C; (g) SEM of glass bead's section from residue; (h) EDS of point D.

EDS, as shown in Fig. 6. Based on the EDS results in Fig. 6b, d, it can be predicted that Al existed in the surface and inside glass beads, and the percentage of Al inside (point B) glass beads was abundant similarly. As Fig. 6e shows, the glass beads appear to be corroded by sulfuric acid, and the structures of grooves/holes were formed.

The EDS results show that the percentage of Al on the surface of the glass beads dramatically decreased from 35.72 (point A) to 5.72% (point C) during the pressure leaching by H_2SO_4 , which indicates that after H_2SO_4 leaching, the Al on the surface was dissolved by the acid. After acid leaching, the grooves and holes were observed in the cross-section of the glass beads (Fig. 6g). In other words, sulfuric acid entered inside the glass beads and reacted with Al, but it did not completely dissolve Al because the EDS results show that the Al content inside the EDS was still as high as 25.11% (point D).

BET Analysis

Based on the analysis of SEM-EDS, it can be predicted that the specific surface area of residue will increase; thus, the area and pore size distributions of the samples were analyzed, and the results are shown in Fig. 2. As expected, few pores (2–5 nm) are observed in the raw CFA, which has a low specific surface area of $2.85 \text{ m}^2 \cdot \text{g}^{-1}$ at models of BET surface area. The pore (2–20 nm) content increased drastically as Al and other metals were extracted from the CFA using the sulfuric acid solution during acid treatment; the result is a sharp increase in the specific surface area from 2.85 to $27.06 \text{ m}^2 \cdot \text{g}^{-1}$. This finding is also consistent with the SEM photos. The surface of particles in fly ash is dense, while that of the particles in leached slag has suffered sulfuric

acid corrosion to form grooves or holes. In addition, the particle size of residue is much smaller than that of CFA.

Leaching Mechanism

Figure 7 shows the dissolution mechanism of Al during sulfuric acid leaching of CFA. As shown before, Al mainly existed in CFA as mullite and amorphous aluminosilicates. However, there was no mullite found in the leaching residue, which indicates that the mullite was completely dissolved during the leaching. Therefore, the further extraction of Al was controlled by the solubility limit of the amorphous aluminosilicates which mainly existed as glass beads in CFA. Sulfuric acid preferentially reacted with Al on the surface of the glass beads during leaching. Although mesoporous pores existed on the surface of the glass beads during leaching, they were not able to create enough pathway for sulfuric acid. In addition, since Al was leached and more Si accumulated on its surface, the pathway of sulfuric acid was further blocked. As a result, the Al extraction could not be improved under experimental conditions.

CONCLUSION

(1) The optimal conditions for the extraction of Al from CFA have been obtained as a sulfuric acid concentration of 3 mol/L, leaching time of 180 min and leaching temperature of 220°C , under which 82.51% of Al could be extracted.

(2) The main chemical composition of leaching residue was SiO_2 , and most of the metals were converted into soluble sulfates and entered into leaching solution.

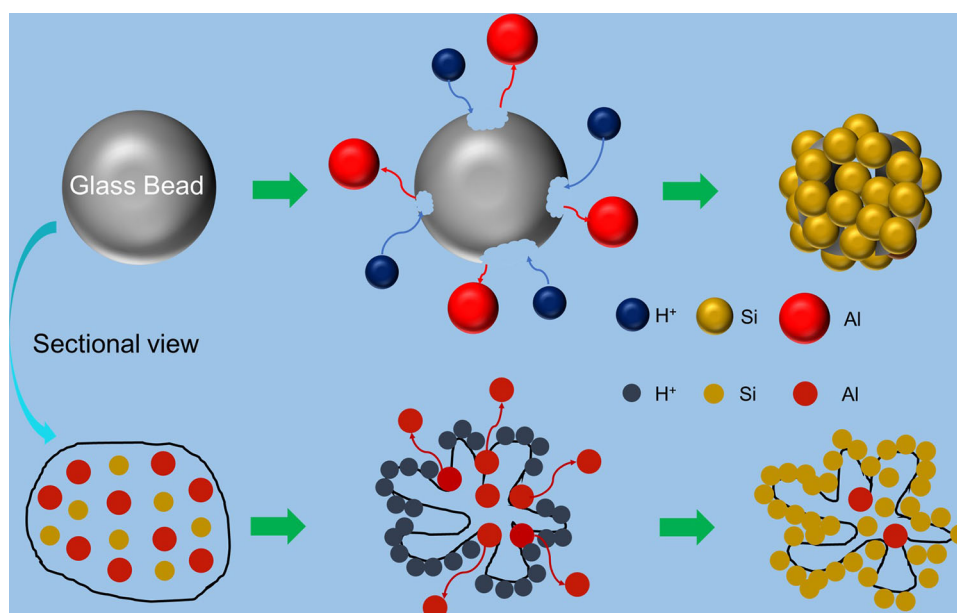


Fig. 7. Simplified diagram of the dissolution mechanism of Al from glass beads during H_2SO_4 leaching.

(3) The mullite ($3\text{Al}_2\text{O}_3 \cdot 2\text{SiO}_2$) in CFA was completely dissolved during leaching. In contrast, sulfuric acid preferentially reacted with Al on the surface of glass beads. With the leaching of Al, more Si was exposed on the beads' surface. As a result, the pathway of sulfuric acid was blocked, which inhibited the further extraction of Al.

ACKNOWLEDGEMENTS

The authors thank the Testing Center of Fuzhou University for the help with the elemental analysis presented in this study.

CONFLICT OF INTEREST

The authors declare that they have no conflict of interest.

REFERENCES

- Z.Y. Yao, M.S. Xia, P.K. Sarker, and T. Chen, *Fuel* 120, 74. (2014).
- V. Manoharan, I.A.M. Yunusa, P. Loganathan, R. Lawrie, C.G. Slibck, M.D. Burchett, B.R. Murran, and D. Eamus, *Fuel* 89(11), 3498. (2010).
- R.S. Blissett, and N.A. Rowson, *Fuel* 97, 1. (2012).
- K. Sobolev, I.F. Vivian, R. Saha, M.W. Nazimuddin, and E.S. Nibert, *Fuel* 116, 471. (2014).
- L. Zeng, H.J. Sun, T.J. Peng, and W.M. Zheng, *Waste Manage.* 106, 184. (2020).
- E.R. Teixeira, A. Camoes, F.G. Branco, J.B. Aguiar, and R. Fanguero, *Waste Manage.* 94, 39. (2019).
- X.M. Liu, X.B. Zhao, H.F. Yin, J.L. Chen, and N. Zhang, *J. Hazard. Mater.* 349, 262. (2018).
- M.P. Kuzmin, L.M. Larionov, V.V. Kondratiev, M.Y. Kuzmina, V.G. Grigoriev, and A.S. Kuzmina, *Constr. Build. Mater.* 179, 117. (2018).
- Q.M. Ma, R.X. Guo, Z.M. Zhao, Z.W. Lin, and K.C. He, *Constr. Build. Mater.* 93, 371. (2015).
- J. Ding, S.H. Ma, S. Shen, Z.L. Xie, and Y. Zhang, *Waste Manage.* 60, 375. (2017).
- Z.Q. Jiang, X. Yang, H.W. Ma, L. Wang, and X. Ma, *Trans. Nonferrous Metals Soc. China* 25(6), 2065. (2015).
- X.B. Li, H.Y. Wang, Q.S. Zhou, T.G. Qi, G.H. Liu, and Z.H. Peng, *JOM* 72, 3341. (2020).
- G.H. Bai, W. Teng, X.G. Wang, J.G. Qin, P. Xu, and P.C. Li, *Trans. Nonferrous Metals Soc. China* 20(1), 169. (2010).
- R.H. Matjie, J.R. Bunt, and J.H.P.V. Heerden, *Mine. Eng.* 18(3), 299. (2005).
- C.B. Guo, J.J. Zou, C.D. Wei, and Y.S. Jiang, *Energy Fuels* 27(12), 7868. (2013).
- V. Kaplan, N. Dosmukhamedov, E. Zholdasbay, G. Daruesh, and A. Argyn, *JOM* 72, 3348. (2020).
- M.C. Tang, C.C. Zhou, J.H. Pan, N.N. Zhang, C. Liu, S.S. Cao, T.T. Hua, and W.S. Ji, *Mine. Eng.* 136, 36. (2019).
- R.K. Taggart, J.C. Hower, and H.K. Heileen, *Int. J. Coal Geol.* 196, 106. (2018).
- Y.X. Guo, Y. Li, F. Cheng, M. Wang, and X.W. Wang, *Fuel Process. Technol.* 110, 114. (2013).
- Z.B. Ma, S. Zhang, H.R. Zhang, and F.Q. Cheng, *J. Clean. Prod.* 230, 302. (2019).
- G.H. Bai, Y.H. Qiao, B. Shen, and S.L. Chen, *Fuel Process. Technol.* 92(6), 1213. (2011).
- A. Shemi, R.N. Mpana, S. Ndlovu, L.D.V. Dyk, V. Sibanda, and L. Seepe, *Mine. Eng.* 34, 30. (2012).
- A. Shemi, S. Ndlovu, V. Sibanda, and L.D.V. Dyk, *Hydrometallurg* 157, 348. (2015).
- C.Y. Wu, H.F. Yu, and H.F. Zhang, *Trans. Nonferrous Metals Soc. China* 22(9), 2282. (2012).
- C.D. Wei, S. Cheng, F.J. Zhu, X.L. Tan, W.Q. Li, and P.P. Zhang, *Hydrometallurgy* 180, 41. (2018).
- D. Valeev, I. Kuniilova, A. Alpatov, A. Mikhailova, and M. Goldberg, *J. Clean. Prod.* 218, 192. (2019).
- A.K. Tripathy, C.K. Sarangi, B.C. Tripathy, K. Sanjay, I.N. Bhattacharya, B.K. Mahapatra, P.K. Behera, and B.K. Satpathy, *Int. J. Miner. Process.* 138, 44. (2015).
- S. Alexander, P. Andrey, A. Suss, Y. Layner, *Light Metals*, 203 (2013).
- Y. Kuroki, N. Iwata, T. Hatsuse, T. Okamoto, M. Takata, and I.O.P. Conf, *Ser. Mater. Sci. Eng.* 21, 012004. (2011).
- Q.S. Wang, *J. Tianjin Univ. Technol.* 2, 40. (1986).
- H. Li, G. Kuang, S. Hu, R. Jin, and R.L. Vekariya, *JOM* 68(10), 2653. (2016).
- H. Guo, G. Kuang, J.X. Yang, and S. Hu, *Meatall. Mater. Trans. B* 47(6), 3557. (2016).

Publisher's Note Springer Nature remains neutral with regard to jurisdictional claims in published maps and institutional affiliations.